Scintillator based energetic ion loss diagnostic for the National Spherical Torus Experiment

D. S. Darrow
Princeton Plasma Physics Laboratory, Princeton, New Jersey 08543-0451, USA

(Received 29 August 2007; accepted 2 December 2007; published online 5 February 2008)

A scintillator based energetic ion loss detector has been built and installed on the National Spherical Torus Experiment (NSTX) [Synakowski *et al.*, Nucl. Fusion **43**, 1653 (2000)] to measure the loss of neutral beam ions. The detector is able to resolve the pitch angle and gyroradius of the lost energetic ions. It has a wide acceptance range in pitch angle and energy, and is able to resolve the full, one-half, and one-third energy components of the 80 keV D neutral beams up to the maximum toroidal magnetic field of NSTX. Multiple Faraday cups have been embedded behind the scintillator to allow easy absolute calibration of the diagnostic and to measure the energetic ion loss in several ranges of pitch angle with good time resolution. Several small, vacuum compatible lamps allow simple calibration of the scintillator position within the field of view of the diagnostic's video camera. © *2008 American Institute of Physics.* [DOI: 10.1063/1.2827514]

I. INTRODUCTION

Magnetically confined fusion plasmas are often heated by energetic ions, be they neutral beam ions, ion cyclotron heated tail ions, or deuterium-tritium (DT) fusion produced alpha particles. For efficient plasma heating, good confinement of the energetic ions is required. Conversely, a large loss rate of energetic ions can cause localized heating of the plasma facing wall components, possibly causing damage or pollution of the plasma. In addition, details of any loss often reveal aspects of the physical processes that induced the loss. For all these reasons, it is desirable to measure the loss rate of energetic ions from these plasmas and understand the processes that produce fast ion loss in the eventual hope of mitigating or eliminating those losses.

Energetic ion losses can be measured by a number of means, including Faraday cups,[2–4] surface barrier diode detectors,[5–9] track detectors,[10] exposure samples,[11–14] infrared imaging,[15] and scintillator,[16–26] and calorimeter probes.[27] Scintillator detectors have the advantage that they can provide the pitch angles and energies of the lost ions as a function of time during a discharge. Knowing these quantities, and the magnetic structure of the discharge, it is possible to reconstruct the loss orbits, which aid significantly in understanding the mechanisms of loss. Consequently, a scintillator detector was chosen for installation in the National Spherical Torus Experiment[1] (NSTX), and has been designated "sFLIP" which stands for "scintillator fast lost ion probe." (The prefix "s" distinguishes this instrument from the "iFLIP," the "interim fast lost ion probe" that used Faraday cups to detect fast ion loss and which was installed for the initial neutral beam operation in NSTX in 2000.)

A scintillator detector relies upon the geometry of the plasma's magnetic field, aperture positions, and scintillator location to disperse the lost energetic ions in energy and pitch angle. Fast ions striking the scintillator plate produce a pattern of light indicating the distribution of ions lost at the detector position. In this work, the pitch angle of a particle is defined as $\chi=\arccos(v_\parallel/v)$, where $v_\parallel$ is the component of the particle's velocity along the local magnetic field. The gyroradius is taken to be $\rho=mv/qB$, which is effectively a measure of the particle's energy. Figure 1 depicts the principle of operation of a scintillator detector. Detectors of this sort have also been used on the TFTR,[16,17] CHS,[18,19] W-7AS,[20] LHD,[21] JFT-2M,[22] JET,[23,24] and ASDEX-U (Ref. 25 and 26) experiments. Because of the geometry of detection, the size of the detector must be about a fast ion gyroradius. For the typical 80 keV deuterium neutral beam ions near the outer midplane of NSTX, that gyroradius is about 30 cm. Scintillator detectors in some of the experiments listed above have had the scintillation light coupled directly to a video camera by a single lens. Since an image-preserving quartz fiber optic bundle was available, it was decided to carry the scintillator image to the camera through the bundle, allowing the video camera to be at a greater distance (up to 8 m) from the magnetic fields, electrical noise, and radiation produced by NSTX. That arrangement is shown schematically in Fig. 2.

II. DESIGN GOALS AND CONSTRAINTS

The design goals of this detector were to (1) detect cogoing fast ion loss over as wide a range of pitch angles as possible; (2) distinguish between the loss of ions at the full (80 keV), one-half (40 keV), and one-third (27 keV) beam energy at the same pitch angle and at the highest NSTX design toroidal field strength of 0.6 T; and (3) resolve pitch angle to $\pm 3°$. In addition, the design needed to include means for simple calibration of the absolute flux of fast ions to the detector and of the position of the scintillator in the videocamera field of view.

Constraints for this detector were that it cannot be placed on the midplane, due to conflict with the lines of sight of other NSTX diagnostics, that it can be dismountable for manned vessel entry through the port where it is located, and that it maintains the scintillator temperature below 200 °C for neutral beam and plasma heat loads lasting up to 5 s, the

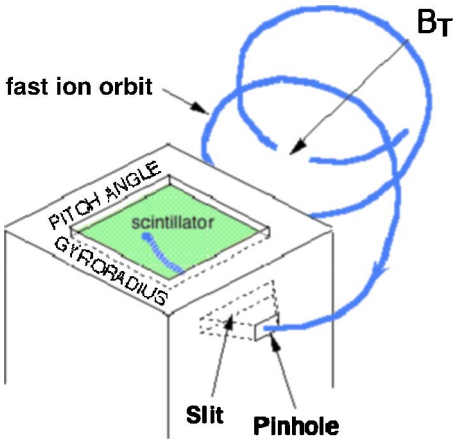

FIG. 1. (Color online) Principle of operation of a scintillator-type fast ion loss detector. The pinhole and slit behind it, in the side of the detector, with the intrinsic magnetic field of the plasma, constrain fast ions of certain gyroradii and pitch angle to strike the scintillator at certain positions, acting as a magnetic spectrometer. The pattern of luminosity produced by the distribution of fast ions incident upon the scintillator is then imaged by an optical system and videocamera to record the time variation of the loss.

maximum neutral beam pulse length in NSTX. This temperature limit was chosen as it is the limit above which the luminosity of the chosen scintillator [P46, yttrium aluminum garnet (YAG):Ce] begins to diminish with increasing temperature.[28] It was also desired to be able to change the scintillator plate in the probe with only in-vessel access and without complete removal of the probe from the vessel. Similarly, it was desired to be able to replace the aperture assembly without removal of the probe from the vessel.

III. DESCRIPTION

A photograph of the principal components of the probe is shown in Fig. 3, and Fig. 4 is a photograph of the probe assembly. Figure 5 shows the probe assembly mounted inside the NSTX vacuum vessel.

The probe consists of a large, thick rectangular copper frame that is brazed onto a thick copper supporting foot. The structure of the probe was built largely from copper to insure good conduction of plasma-deposited heat away from the scintillator, in order to keep the scintillator material at a temperature insuring constant luminous response. A large stainless steel supporting strap was welded to the inside of the

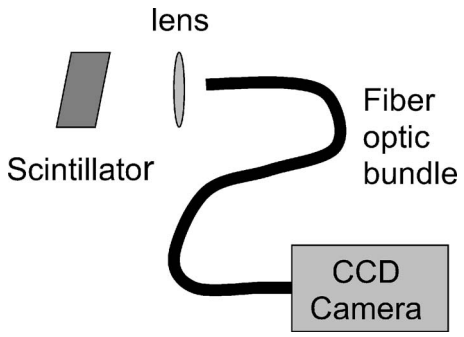

FIG. 2. Sketch of optical train of the diagnostic, including scintillator plate, focusing lens, image-preserving fiber optic bundle, and CCD video camera. Image sequences from the CCD camera are captured digitally for storage, review, and analysis.

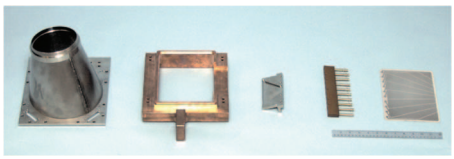

FIG. 3. (Color) Exploded view of the sFLIP in-vessel components, showing (left to right) the conical light shield, copper frame, aperture block, Faraday cup spring contact assembly, and the scintillator plate. A 30 cm ruler is show below the scintillator plate for scale.

NSTX vacuum vessel to support the probe foot, with four 25 mm diameter bolts to press the foot against the vessel wall for the best possible thermal transfer to the vessel. Allowance was also made for attachment of water cooling tubes to the exterior of the vacuum vessel directly outside the position of the foot, in order to provide further ability to keep the scintillator cool. However, the period of initial operation of the probe demonstrated that, even with no cooling, the scintillator temperatures were never reaching anywhere beyond a few degrees above room temperature. Consequently, the external cooling tubes were never installed. Because of the large size of the copper frame, its high conductivity material, and its proximity to the plasma, engineering calculations were performed to ensure that it would not be damaged by eddy current forces during possible plasma disruptions or other sudden changes in magnetic fields near the probe. The design was determined to be fully adequate for the worst case scenarios modeled. Indeed, the in-vessel structure has endured nearly four years and 15 000 plasma pulses without apparent mechanical or thermal damage.

The copper frame of the probe is inclined by 11.25° from vertical to match the shape of the high harmonic fast wave antennas and associated limiters in NSTX. This inclination is visible in Fig. 4. The front aperture of the probe has a height of 12.0 mm and width of 2.0 mm, and is 138.4 mm from the center of the scintillator plate. The rear aperture of the probe has a height of 103.2 mm and a width of 2.0 mm, and is located 76.8 mm from the center of the scintillator plate. The

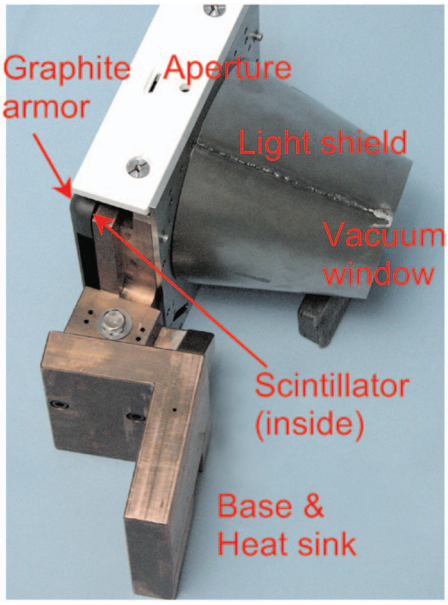

FIG. 4. (Color) Photograph of the sFLIP assembly

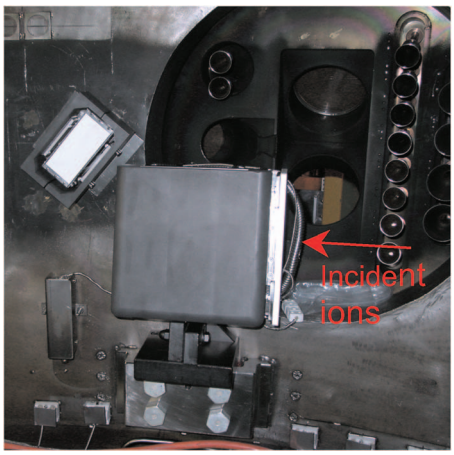

FIG. 5. (Color) Photograph of the sFLIP inside the NSTX vacuum vessel.

line through the centers of the apertures is parallel to the surface of the scintillator plate, but is displaced 14.0 mm toward the vacuum window from the coated plate surface. The apertures are centered along the 20 cm wide side of the scintillator plate. After installation, the front aperture center location was measured with a mechanical measuring arm inside the NSTX vacuum vessel and was found to lie at a major radius of 1.603 m and a vertical position of 0.1422 m below the machine's equatorial plane.

The lost ions are detected by way of the luminosity they create when they strike the scintillator plate, and the resulting luminous pattern is recorded by a video camera. Because the plasma itself can be a bright source of light, the probe structure includes a conical light shield, blackened on the inside to eliminate reflections. This shield excludes plasma light from entering the probe structure. The end of the conical shield opposite the scintillator fits snugly into the vacuum side of a 117 mm diameter Conflat fused silica vacuum window. The aperture pair that admits the fast ions to the probe is arranged in such a way that there is no direct line of sight through the apertures to the scintillator plate, thus preventing light entering from outside the probe from reaching the scintillator plate and being mistakenly interpreted as fast ion loss.

IV. CALIBRATION AND RESULT INTERPRETATION

The luminescent pattern on the scintillator is determined by the aperture dimensions, their position relative to the scintillator plate, and the local magnetic field direction and strength. Interpretation of the images from the camera requires knowledge of the location of the edges of the scintillator within the camera field of view. This location calibration is accomplished with several miniature incandescent light bulbs mounted inside the copper frame of the probe, such that they illuminate the corners of the scintillator and the image of the lamp light diffusely scattered by the scintillator coating can be recorded on the video camera. This is very similar to the calibration method previously used in the CHS scintillator probe,[19] and the bulbs used are of the same kind. Discretization of the image, owing to the fact that the fiber optic bundle is only 50×50 fibers, introduces only a small uncertainty in the position calibration. There are some broken fibers in the bundle, but the number of broken fibers is small enough that it does not place any significant restriction on the interpretation of images from the probe. In the work reported here, a Xybion ISG-250-R-3 charge coupled device (CCD) video camera with an image intensifier in front of the CCD sensor was used. This camera produced NTSC (National Television Standards Committee) video output with 60 fields per second. The light from the fiber optic bundle was proximity coupled to the 1 in. format intensifier by placing the end of the bundle in direct contact with the input face of the intensifier. A digital frame grabber was used to capture the sequence of camera images over the course of each plasma.

For quantitative interpretation of the camera images, grids of pitch angle and gyroradius centroid are computed for each case of interest using the grid calculation program (NL_DETSIM, aka NLSDETSIM) (Ref. 16) used for the TFTR lost alpha diagnostic and the CHS and LHD fast ion loss probes. This program applies the dimensions and relative locations of the apertures, scintillator plate, and local magnetic field to launch and follow ion orbits inside the probe, tallying, by gyroradius and pitch angle, where they strike the scintillator plane. This program assumes that the ion orbits are perfect mathematical helices, and launches, for each gyroradius and pitch angle pair, hundreds or thousands of orbits with initial positions distributed across the full extent of the front aperture. The centroid of the strike points for all particles started at a given pitch angle, and gyroradius defines the grid position for that value of gyroradius and pitch angle. The calculated centroid locations overlaid exactly with the centroids calculated by the code "EFIPDESIGN" used in the design of the probe for the W7-AS device.[20] For stellarators such as CHS, LHD, or W7-AS where the magnetic field is essentially fully determined by magnetic field coil currents, and for conventional tokamaks where the dominant magnetic field is that created by the toroidal field coils (TFTR and JFT-2M), the magnetic field direction varies only a little from one plasma condition to another. In such cases, the gyroradius and pitch angle interpretation grids may have little or no perceptible variation between different plasma conditions. In the spherical tokamak plasmas in NSTX, however, the poloidal magnetic field can equal or exceed the toroidal field strength at the probe location. Consequently, the local field line direction at the probe can vary from entirely horizontal at the beginning of the discharge when the toroidal field is on but the plasma current is zero, to as much as 50° inclined from horizontal when the plasma current is at its maximum value. Consequently, an entire library of pitch angle and gyroradius interpretation grids is needed for the sFLIP diagnostic. The appropriate grid to use for any given loss image is determined by calculating the magnetic field direction at the probe location from the magnetic equilibrium (computed by the EFIT code[29]), and choosing the grid for that field line angle from the library of grids.

Absolute calibration of the flux of fast ions in a scintillator probe can be performed by measurement of the phosphor's luminous response to energetic ions from an accelerator and measurement of the camera's intensity signal for an

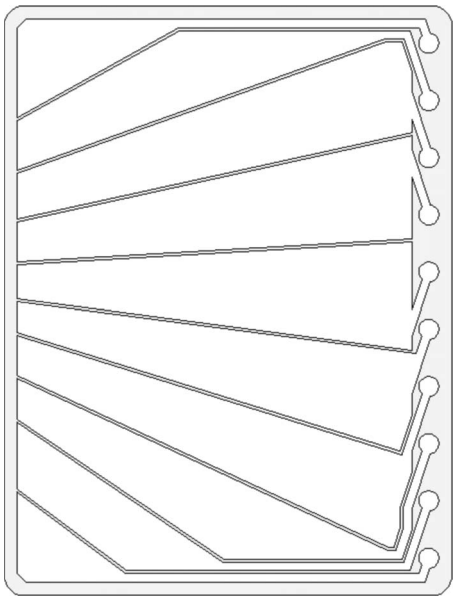

FIG. 6. Drawing of the Faraday cup strip pattern on the phosphor substrate. The plate is 15.0×20.0 cm and the apertures lie at the edge of the plate where the tapered strips converge The strips are numbered from 1 to 10 running from top to bottom in this image, extending from lowest to highest pitch angles, correspondingly.

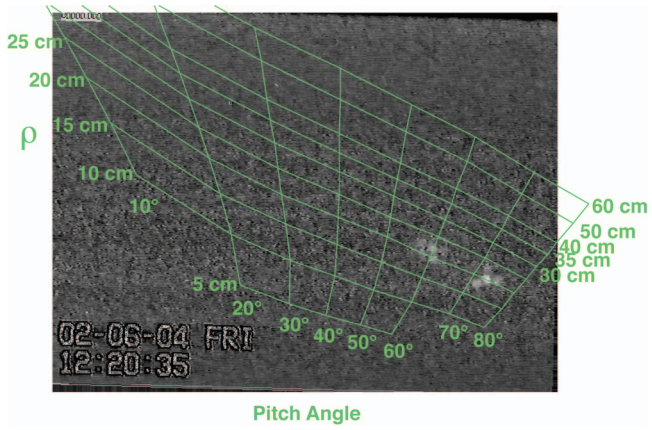

FIG. 7. (Color) Fast ion loss image from NSTX shot 111192 at 253 ms. The image is overlaid with a grid in pitch angle and gyroradius centroid for interpretation. Note the two luminous spots registered toward the right edge of the image. These arise from neutral beam ions being lost at two different pitch angles and then striking the scintillator.

extended luminous source at the phosphor's emission wavelength, placed at the scintillator location. In practice, though, the several steps required to transfer the responses can result in significant uncertainties in the calibration obtained. For the NSTX probe, an alternate absolute calibration technique has been adopted. The fast ion current coming to the metalized strips coated on the scintillator substrate is measured. The strip shapes are shown in Fig. 6 and the segments can also be seen on the scintillator substrate shown in Fig. 3. The scintillator substrate plate is 15.0×20.0 cm and the apertures lie at the edge of the plate where the tapered strips converge. The shape of the strips correspond to 10° wide bins in pitch angle for a model 1 MA plasma equilibrium in NSTX. For plasma magnetic equilibria that differ from that used as the design basis, the strips will deviate from covering those exact bins in pitch angle, but the total current received by all strips can be used as an absolute calibration for the total intensity in the camera image, thus allowing a complete calibration of the image. The phosphor substrate plate is a bonded mica flake sheet approximately 1 mm thick. The Faraday cup strips were metalized with ~1 micron thick vapor deposited aluminum. There is a 1 mm wide uncoated gap between strips. While most of the plate is over coated with a powdered scintillator layer (P46, YAG:Ce), the circular lands along the right edge of the plate, as viewed in Fig. 6, are left uncoated so that good electrical contact can be maintained to the Faraday cup strips with the spring loaded contact pins shown in Fig. 3. The choice of P46 for the phosphor was motivated by its durability, linearity over a wide range of fluxes, and essentially constant response over the expected temperature range of operation (20–150 °C).[25]

The method of absolute calibration using Faraday cups was first utilized in the scintillator probes in CHS (Ref. 19) and W7-AS.[20] It relies on the assumption that the charge deposited by fast ions that strike the scintillator will take the nearby low-resistance return path provided by the metallized strips under the phosphor powder coating, rather than diffusing through the insulating phosphor powder or substrate layers. The metalized strips, essentially Faraday cups, are connected electrically to current-to-voltage amplifiers in an instrument rack outside the vacuum vessel. These amplifiers hold their inputs at a virtual ground potential, equal to the vacuum vessel potential. The fast ions striking the scintillator surface can, in principle, generate secondary electrons. However, any such secondary electrons generated will have only a few eV of energy.[30] The volume inside the metallic probe assembly is an equipotential, so there are no electric fields to accelerate any secondary electrons produced. Since the magnetic field strength in the interior of the probe is ~0.2 T for typical NSTX conditions, a secondary electron with an energy of 10 eV will have a gyroradius of only ~0.05 mm, There will therefore be no significant spatial displacement of any secondary electrons generated, and they should simply orbit in the magnetic field back to within a gyroradius of the point where they were born, causing no significant deviation in the Faraday cup currents.

V. INITIAL RESULTS

Figure 7 shows a scintillator image from NSTX shot 111192 (I_p=800 kA and B_T=0.3 T) at 253 ms. This image is overlaid with a grid in pitch angle and gyroradius centroid for interpretation. Note the two luminous spots registered toward the right edge of the image. These result from neutral beam ion loss at two different pitch angles. In this discharge, the neutral beam was injected at an energy of 91.5 keV, and the magnetic field at the probe position was 0.301 T, giving a gyroradius of 20.0 cm for the full energy deuterium beam ions. This is in good agreement with the observed gyroradius for both spots as both lie virtually centered on the 20 cm grid line. The localization of the luminous spots confirms that they are due to fast ions striking the scintillator and not to plasma light leaking into the probe enclosure, which would provide more diffuse illumination. Additional confirmation that no plasma light is being seen by the CCD camera is provided during Ohmically heated plasmas in NSTX. During

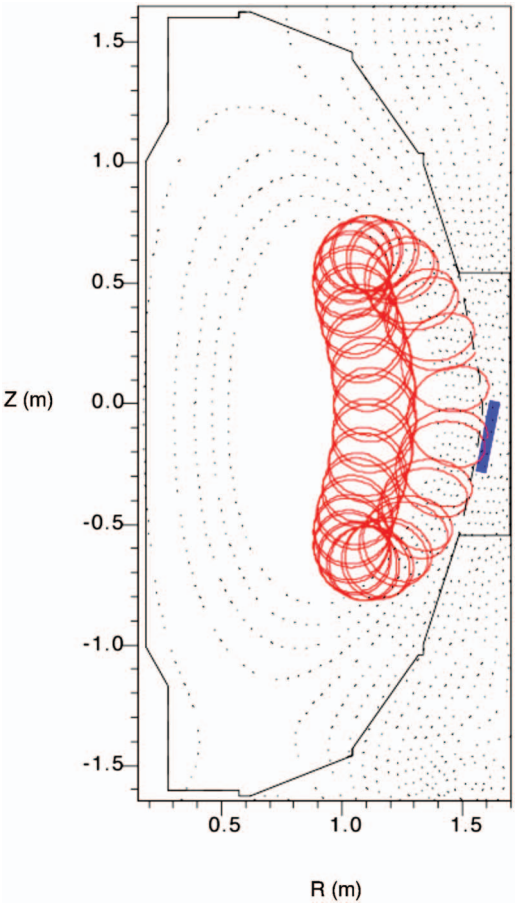

FIG. 8. (Color) A projection of the NSTX plasma facing components (solid and long dash black lines), the sFLIP detector (blue rectangle), plasma flux surfaces (dotted lines), and the orbit of the 91.5 keV deuteron at a pitch angle of 73° (red) from the case shown in Fig. 7.

these shots, there is plasma produced light all throughout the vacuum chamber, but no population of fast ions. In such discharges, no light is seen in the camera image. Each of the luminous regions seen in Fig. 7 is visibly subdivided into multiple small circular spots. These are the individual optical fibers that transmit the image to the camera. This discretization introduced by the individual fibers broadens slightly the instrumental response function arising from the aperture dimensions but still allows essentially all of the useful information in the image to be extracted. Figure 8 shows the reconstructed orbit of a 91.5 keV deuteron coming to the detector at a pitch angle of 73° in the magnetic equilibrium for shot 111192 at 253 ms, which would produce the luminous spot on the right of the image in Fig. 7.

ACKNOWLEDGMENTS

Engineering design and analysis by G. Labik, F. Dahlgren, and D. Card are gratefully acknowledged, as is extensive technical work by D. Card and D. LaBrie. The considerable assistance with the digital video acquisition system given by W. Davis is greatly appreciated. Project management aid from S. Schoen was invaluable. Logistical support from A. L. Roquemore was indispensable. Interest and encouragement from M. Ono and D. Johnson are much appreciated. Helpful conversations with S. Zweben are acknowledged. This work was supported by U.S. DOE Contract No. DE-AC02-76-CH03073.

[1] J. Spitzer, M. Ono, M. Peng, D. Bashore, T. Bigelow, A. Brooks, J. Chrznowski, H. M. Fan, P. Heitzenroeder, T. Jarboe, R. Kaita, S. Kaye, H. Kugel, R. Majeski, C. Neumeyer, R. Parsells, E. Perry, N. Pomphrey, J. Robinson, D. Strickler, and R. Wilson, Fusion Technol. **30**, 1337 (1996).
[2] W. W. Heidbrink, M. Miah, D. Darrow, B. LeBlanc, S. S. Medley, A. L. Roquemore, and F. E. Cecil, Nucl. Fusion **43**, 883 (2003).
[3] W. P. West, C. J. Lasnier, J. Watkins, J. S. deGrassie, W. Heidbrink, K. H. Burrell, and F. E. Cecil, J. Nucl. Mater. **337–339**, 420 (2005).
[4] O. N. Jarvis, P. van Belle, G. Sadler, G. A. H. Whitfield, F. E. Cecil, D. Darrow, and B. Esposito, Fusion Technol. **39**, 84 (2001).
[5] R. E. Chrien, R. Kaita, and J. D. Strachan, Nucl. Fusion **23**, 1399 (1983).
[6] W. W. Heidbrink, J. Lovberg, J. D. Strachan, and R. E. Bell, Nucl. Fusion **27**, 129 (1987).
[7] H.-S. Bosch and U. Schumacher, "Controlled Fusion and Plasma Heating," *Proceedings of the 13th European Conference, Schliersee, 1986* (European Physical Society, Geneva, 1986), Vol. 10C, Part II, p. 124.
[8] J. D. Strachan, Nucl. Fusion **29**, 163 (1989).
[9] G. Martin, O. N. Jarvis, and J. Kallne, Phys. Scr., T **T16**, 171 (1987).
[10] T. D. Murphy and J. D. Strachan, Nucl. Fusion **25**, 383 (1985).
[11] R. A. Langley, Bull. Am. Phys. Soc. **29**, 1309 (1984).
[12] E. V. Caruthers, J. Zhu, P. C. Stangeby, G. M. McCracken, J. P. Coad, S. K. Erents, D. H. J. Goodall, J. C. B. Simpson, and J. W. Partridge, J. Nucl. Mater. **176/177**, 1027 (1990).
[13] J. Zhu, G. M. McCracken, and J. P. Coad, Nucl. Instrum. Methods Phys. Res. B **59/60**, 168 (1991).
[14] H. W. Herrmann, S. J. Zweben, D. S. Darrow, J. R. Timberlake, G. P. Chong, A. A. Haasz, C. S. Pitcher, and R. G. Macaulay-Newcombe, Nucl. Fusion **37**, 293 (1997).
[15] K. Tobita, Y. Neyatani, Y. Kusama, and H. Takeuchi, Rev. Sci. Instrum. **66**, 594 (1995).
[16] S. J. Zweben, R. L. Boivin, M. Diesso, S. Hayes, H. W. Hendel, H. Park, and J. D. Strachan, Nucl. Fusion **30**, 1551 (1990).
[17] D. S. Darrow, H. W. Herrmann, D. W. Johnson, R. J. Marsala, R. W. Palladino, and S. J. Zweben, Rev. Sci. Instrum. **66**, 476 (1995).
[18] D. S. Darrow, M. Isobe, T. Kondo, M. Sasao, K. Toi, M. Osakabe, K. Matsuoka, S. Okamura, S. Kubo, C. Takahashi, and the CHS Group, *Proceedings of the Joint Conference of the 11th International Stellarator Conference and 8th International Toki Conference on Plasma Physics and Controlled Nuclear Fusion, 1997* (Japan Society of Plasma Science and Nuclear Fusion Research, Nagoya, Japan, 1998), Vol. 1, p. 362.
[19] D. S. Darrow, M. Isobe, T. Kondo, M. Sasao, and the CHS Group, Rev. Sci. Instrum. **70**, 838 (1999).
[20] D. S. Darrow, A. Werner, and A. Weller, Rev. Sci. Instrum. **72**, 2936 (2001).
[21] M. Nishiura, M. Isobe, T. Saida, M. Sasao, and D. S. Darrow, Rev. Sci. Instrum. **75**, 3646 (2004).
[22] K. Shinohara, H. Kawashima, K. Tsuzuki, K. Urata, M. Sato, H. Ogawa, K. Kamiya, H. Sasao, H. Kimura, S. Kasai, Y. Kusama, Y. Miura, K. Tobita, O. Naito, the JFT-2M Group, and D. S. Darrow, Nucl. Fusion **43**, 586 (2003).
[23] S. Baeumel, A. Werner, R. Semler, S. Mukherjee, D. S. Darrow, R. Ellis, F. E. Cecil, L. Pedrick, H. Altmann, V. Kiptily, and J. Gafert, Rev. Sci. Instrum. **75**, 3563 (2004).
[24] S. D. Pinches, V. G. Kiptily, S. E. Sharapov *et al.*, Nucl. Fusion **46**, S904 (2006).
[25] M. Garcia-Muñoz, "Fast response scintillator based detector for MHD induced energetic ion losses in ASDEX Upgrade," PhD Thesis Ludwid-Maximillian-University of Munich, 2006.
[26] M. Garcia-Muñoz, P. Martin, H.-U. Fahrback, M. Gobbin, S. Günter, M. Maraschek, L. Marrelli, H. Zohm, and the ASDEX Upgrade Team Nucl. Fusion **47**, L10 (2007).
[27] D. M. Manos, R. V. Budny, S. Kilpatrick, P. Stangeby, and S. Zweben, Rev. Sci. Instrum. **57**, 2107 (1986).
[28] M. Tuszewski and S. Zweben, Rev. Sci. Instrum. **64**, 2459 (1993).
[29] L. Lao, H. St. John, R. D. Stambaugh, A. G. Kellman, and W. Pfeiffer, Nucl. Fusion **25**, 1611 (1985).
[30] K. E. Pferdekämper and H.-G. Clerc, Z. Phys. A **275**, 223 (1975).